ISSN 1996-3343

Asian Journal of Applied Sciences

http://knowledgiascientific.com

Knowledgia SCIENTIFIC
A Place to Publish Outstanding Research

Asian Journal of Applied Sciences 9 (1): 13-22, 2016
ISSN 1996-3343 / DOI: 10.3923/ajaps.2016.13.22

Characterization of Spray Deposited $ZnMn_2O_4$ Nanostructured Thin Films

[1]Rini S. Hanna Scarlet, [2]S. Sriram and [2]D. Balamurugan
[1]Centre for Nanotechnology and Advanced Biomaterial (CeNTAB), School of Electrical and Electronics Engineering, SASTRA University, Tirumalaisamudram, Thanjavur, 613401, India
[2]School of Electrical and Electronics Engineering, SASTRA University, Tirumalaisamudram, Thanjavur, 613401, India

Corresponding Author: D. Balamurugan, School of Electrical and Electronics Engineering, SASTRA University, Tirumalaisamudram, Thanjavur 613401, India

ABSTRACT

In this study, the undoped MnO_2 was deposited using spray pyrolysis technique. The manganese (II) acetate tetra hydrate was taken as 0.1M. The film was then annealed at 450°C for 5 h to obtain crystalline peak. The XRD result for the undoped MnO_2 film shows (110) plane peak with maximum intensity. Optical property shows an increase in transmittance for annealed film and band gap was found to be 2.4 eV. The Electrical property indicates the semiconducting nature of the film. The $ZnMn_2O_4$ film was obtained from aqueous solution manganese (II) acetate tetra hydrate and Zinc acetate dihydrate salt of 0.01:0.01 molar concentration. After annealing the film at 450°C for 5 h, the crystalline peak was observed. The XRD results of $ZnMn_2O_4$ film shows crystalline peaks of (211) and (111) plane. The optical properties shows an increase in transmittance than MnO_2 film. The structural, electrical and morphology properties of the film as a function of annealing temperature were analysed and reported.

Key words: MnO_2 thin films, $ZnMn_2O_4$ thin film, spray pyrolysis

INTRODUCTION

Manganese dioxide is a low band gap, high optical constant semiconductor that exhibits ferroelectric properties (Bhide *et al*., 1959; Koops, 1951). Manganese dioxide (MnO_2) is a widely used material featuring low-cost, high energy density, environmental pollution free and nature abundance (Komaba *et al*., 2008; Ma *et al*., 2008). The principal use of MnO_2 is in dry-cell, alkaline and zinc-carbon batteries. ZnO is a wide-bandgap semiconductor and has several favorable properties, including good transparency, high electron mobility, wide bandgap and strong room-temperature luminescence. Most of the research focuses on the optical properties of ZnO due to its excellent ultraviolet, blue and green light emission (Zu *et al*., 1997; Huang *et al*., 2001; Jin *et al*., 2003; Inoue *et al*., 2006). ZnO is a kind of nontoxic material with good biodegradability and biocompatibility (Zhou *et al*., 2006). ZnO is a promising semiconductor for optical devices due to its nonlinear optical property and excitonic emission at room temperature (Sakohara *et al*., 1992; Kind *et al*., 2002; Look, 2001). The $ZnMn_2O_4$ is a promising functional material and has become the focus of various researches owing to its potential applications. The $ZnMn_2O_4$ could be used for the negative temperature coefficient thermistors on account of their unique electrical properties

(Guillemet-Fritsch *et al*., 2000). Ferraris *et al*. (2002) suggested that $ZnMn_2O_4$ was an efficient catalyst for the reduction of NO to N_2 and, in all cases, its best selectivity to N_2 and CO_2 was at almost the maximum conversion temperature (Fierro *et al*., 2005; Ferraris *et al*., 2002). $ZnMn_2O_4$ has obvious advantages because of its much lower toxicity, cost, and operating voltage (average discharge and charge voltages of 0.5 V and 1.2 V, respectively) compared with the Co or Fe oxides (Yang *et al*., 2008).

There are various techniques are used to deposit the MnO_2 and $ZnMn_2O4$ thin films. They are reactive deposition (Rizzi *et al*., 2000), sol-gel (Long *et al*., 2001; Minami *et al*., 2000), plasma assisted molecular beam epitaxy (Guo *et al*., 2001), r.f. sputtering (Fau *et al*., 1994), thermal decomposition (Farid Ul Islam *et al*., 2005), spray pyrolysis (Farid Ul Islam *et al*., 2007), solid-state reaction (Li *et al*., 1999; Hao *et al*., 2011), co-precipitation method (Zhai *et al*., 2011) and hydrothermal method (Duan *et al*., 2010; Cheng *et al*., 2014). Among the various methods are used to deposit the thin films, in this work spray pyrolysis was used. Spray pyrolysis having many advantages comparing to other deposition techniques. Some of their advantages are; they can cover large area during deposition, low cost and the surface volume ratio can be controlled here. In this work, the undoped MnO_2 and $ZnMn_2O_4$ thin films were deposited on glass substrates and their structural, optical and electrical properties are studied and the results are discussed.

MATERIALS AND METHODS

The materials used for the deposition of undoped MnO_2 and $ZnMn_2O_4$ thin films are Zinc acetate dihydrate ($C_4H_6O_4Zn.2H_2O$) in reagent grade (RA) and Manganese (II) acetate tetra hydrate $(CH_3COO)_2Mn.4H_2O$) in analytical reagent grade. The chemicals were purchased from Sigma Aldrich and Merck and the purity form of Manganese (II) acetate tetra hydrate is >99.5% and for Zinc acetate dihydrate, it is 99.9%.

The undoped MnO_2 thin film samples were deposited by spray pyrolysis technique. The spray solution was prepared from 0.1 M of Manganese (II) acetate tetra hydrate and dissolved in 50 mL of de-ionized water. The thin films were deposited on glass substrate (Labtech Medico (P) Ltd). The distance between the spray gun and substrate was kept at 50 cm. The nozzle angle was kept at 45. The substrate temperature was maintained at 250°C. The solution was sprayed at the glass substrates. The prepared thin films were annealed at 420°C for 5 h.

The $ZnMn_2O_4$ thin films were prepared from the precursor solution containing Zinc acetate dehydrate and Manganese (II) acetate tetra hydrate with 0.01M. The films were deposited on glass substrate (Labtech Medico (P) Ltd). The deposition parameters for undoped MnO_2 and $ZnMn_2O_4$ thin films were given in Table 1. The substrate temperature was maintained at 220°C. The deposited thin films were annealed at 400°C for 5 h to attain the crystalline nature. The deposited

Table 1: Deposition parameters of undoped MnO_2 and $ZnMn_2O_4$

Deposition parameters	Undoped MnO_2	$ZnMn_2O_4$
Precursor salt	Manganese (II) acetate tetra hydrate	Manganese (II) acetate tetra hydrate and Zinc acetate dehydrate
Molarity of precursor salt	0.1M	0.01M
Volume of the solution	50 mL	50 mL
Nozzle angle	45°	45°
Distance between gun and the substrate	50 cm	50 cm
Substrate temperature	250°C	220°C
Spray time between each cycle	15 sec	15 sec
Carrier gas	Compressed air	Compressed air

thin films were allowed to cool on room temperature and then they are used for various studies. During the spray process, compressed air was used as a carrier gas for both films.

The structural properties were characterized by X-ray diffraction (XRD) (D8, Focus Bruker). The optical properties were studied by using UV-Visible-Perkin Elmer make-Model-Lambada 35 (Range 190-1000 nm) spectrophotometer. The surface morphology of the undoped MnO_2 and $ZnMn_2O_4$ films were studied using Atomic Force Microscopy (AFM, Park System, XE170, Germany). The variation in resistance along with the temperature for the undoped MnO_2 thin films was studied using four probe methods. The photoluminescence properties for the deposited undoped MnO_2 and $ZnMn_2O_4$ thin films were studied using photoluminescence spectroscopy.

RESULTS AND DISCUSSION

X-ray diffractometer: The XRD pattern of the undoped MnO_2 and $ZnMn_2O_4$ thin films are shown in Fig. 1. From the diffracted XRD peaks the observed for both the films are found to be

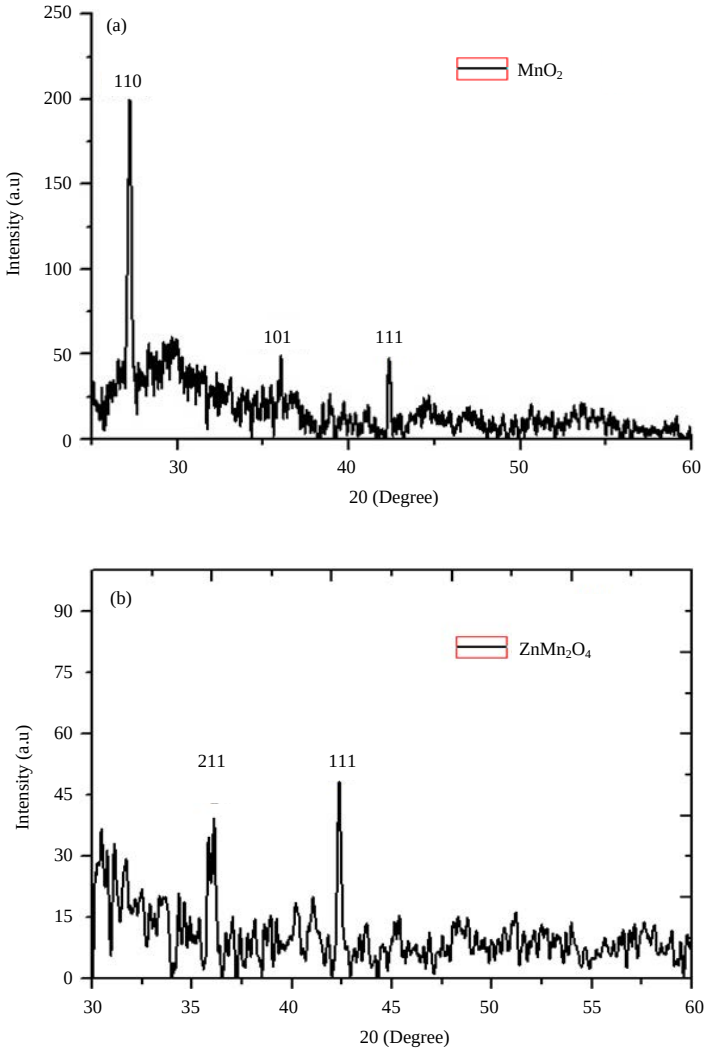

Fig. 1(a-b): (a) XRD pattern for undoped MnO_2 film and (b) XRD pattern for $ZnMn_2O_4$ film

polycrystalline in nature. The phase identification is done by measure d-spacing of obtained diffraction pattern is matched with the standard JCPDS card numbers 24-0735 and 24-1133 for undoped MnO_2 and $ZnMn_2O_4$ films, respectively. The peaks observed for MnO_2 thin film are identified and assigned to the planes (110), (101) and (111) respectively. Similarly, the observed peaks for the $ZnMn_2O_4$ are identified and assigned to (211) and (111) planes. There is no characteristics peak for other elements are observed, which is confirmed by the previous research work done by Xiao *et al*. (2009).

The crystallite size (D) of the samples are calculated using the following equation:

$$D = \frac{K\lambda}{\beta \cos\theta} \tag{1}$$

where, λ is the wavelength, β is the Full width at half maximum intensity and θ is the Bragg angle. The obtained crystallite size for the undoped MnO_2 and $ZnMn_2O_4$ films are 148 and 69 nm, respectively. This result is satisfy the Scherer's formula, were β is inversely proportional to D. The observed D values and FWHM values varies depends due to Zn incorporated with Mn_2O_4.

To identify the crystalline homogeneity, texture of a particular plane, (referred as the deviation from unity used to know plane of preferred growth) can be calculated by following texture co-efficient (TC) Eq. 2.

$$TC_{(hkl)} = \frac{I_{(hkl)} / I_{0(hkl)}}{N^{-1}\sum nI_{(hkl)} / I_{0(hkl)}} \tag{2}$$

where, $I_{(hkl)}$ is measured intensity of a plane (hkl), $I_{o(hkl)}$ is standard intensity of plane (hkl) taken from JCPDS data, N is a reflection number and n is the number of diffraction peaks. $TC_{(hkl)} = 1$, for a sample with random oriented crystal percent's and the larger TCs value is larger abundance of crystallites oriented in (hkl) direction. For the undoped MnO_2 film it is identified as (110) plane which confirms the β-phase of MnO_2(JCPDS card number 24-0735) and is well matched with the earlier reports reported by Zheng *et al*. (2005) and Chandru *et al*. (2012).

Optical properties: The optical properties of deposited films were studied from absorbance and transmittance spectra, recorded by UV-Vis spectrophotometer in the wavelength ranges from 200-1200 nm. The optical absorbance spectrum of undoped MnO_2 and $ZnMn_2O_4$ films are shown in Fig. 2a and b. The optical absorption starts to decrease and this may be due the increased grain size.

Figure 3 shows the comparison of optical transmittance spectrum of MnO_2 films and $ZnMn_2O_4$ films. For both the film samples, the transmittance is obtained in the range of 200-1200 nm. The optical transmittance of MnO_2 samples is found to be upto 40%. This reported value is verified with already existing reports by Farid Ul Islam *et al*. (2005) and it is found to be very low. The reason for the decreasing the transmittance may be due to the preparative condition. However, the transmittance obtained for $ZnMn_2O_4$ thin film is found to be 80%. This may be due to the incorporation of the ZnO component on the MnO_2.

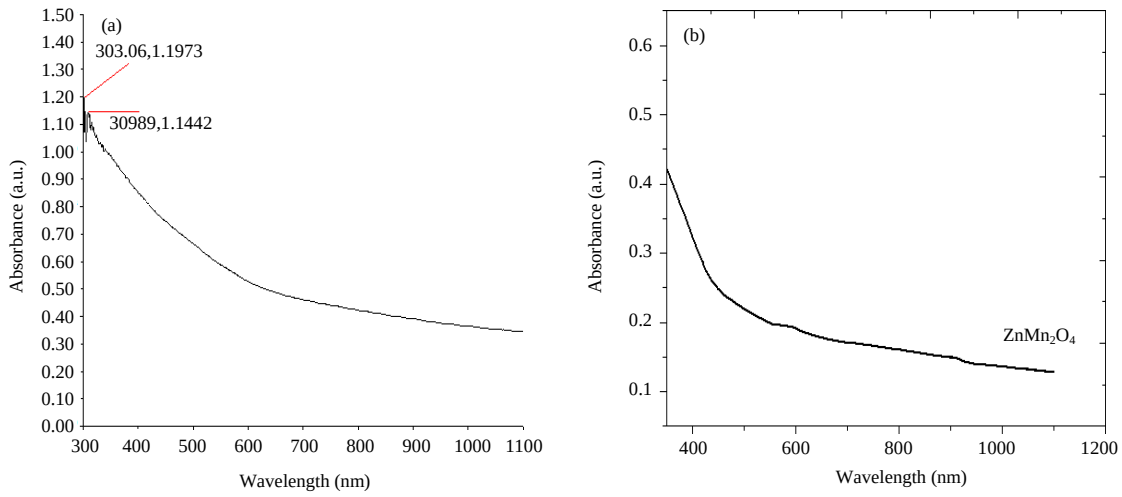

Fig. 2(a-b): Optical absorbance spectrum for (a) MnO_2 film and (b) $ZnMn_2O_4$ film

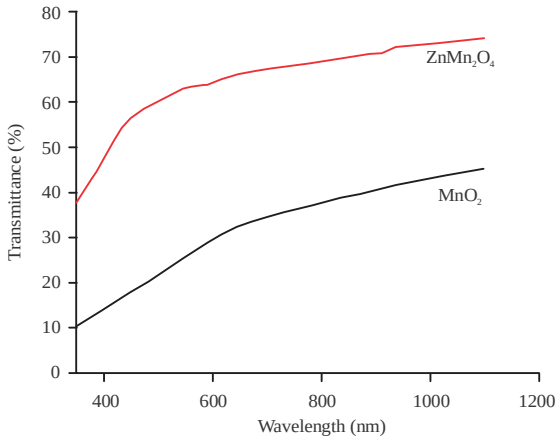

Fig. 3: Comparison of transmittance spectrum between undoped MnO_2 and $ZnMn_2O_4$

Electrical studies: The resistivity for the undoped MnO_2 was calculated by using the following relation:

$$\rho = \frac{V}{I} \times \frac{\pi d}{\ln 2} \tag{3}$$

where, V is the voltage across the crystal, I is the current through the crystal, d is the thickness of the crystal and is the resistivity of the semiconductor. The room temperature electrical studies for the undoped MnO_2 were studied by using four probe methods. Figure 4 shows the electrical properties of the undoped MnO_2 thin films. The resistivity starts to increase with the increase of temperature. This shows the conducting nature of the material, the improvement in crystallinity and grain size induced higher conductivity in sample. The order of resistivity in this study agrees quite well with that of spray-deposited films. However, the resistivity obtained by this method is

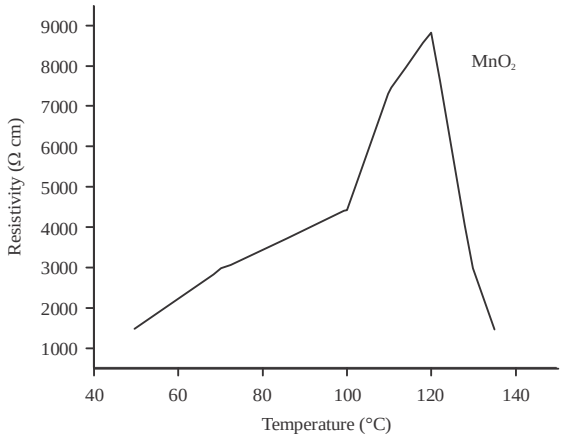

Fig. 4: Resistivity plot for undoped MnO_2 films

so high as compared to the earlier report (Fau *et al*., 1994). This is because of the preparative condition of thin film. After the transition temperature, the resistivity of the material starts to decrease when the corresponding temperature is increased. This region shows the presence of negative temperature coefficient behavior of a semiconductor and the prepared MnO_2 films are semiconducting in nature.

Atomic force microscopy: The morphological study for the undoped MnO_2 was studied by using AFM. The AFM study is used to visualize the surface of the deposited films. The AFM image for undoped MnO_2 thin film is shown in Fig. 5a. The pure MnO_2 morphology indicated a smooth surface with flack like structure covered the entire surface. This may be due to increments of metal nucleation center which resulted to the grain growth towards prose surface from nano flacks structure. From the AFM image, it is evident that the grain size was improved upon annealing treatment. For the deposited MnO_2 films, the surface skewness was found to be -0.5. It is nearly equal to zero. The surface kurtosis for the prepared MnO_2 films was found to be 3.0. From this, we say that the peaks are sharp here.

The AFM image for $ZnMn_2O_4$ thin film is shown in Fig. 5b. From the AFM image, it is evident that the grain size is decreased. The surface skewness for the deposited $ZnMn_2O_4$ films was found to be 0.4. The obtained surface skewness was nearer to zero. The surface kurtosis was found to be 2.98. The obtained surface kurtosis value is approximately equal to three. This shows that they have sharp peak.

The line histogram is a bar graph that shows the distribution of heights along a height profile. It can display the entire range of height of the data points in a line. The width of a bar depends on the overall height range of the sample and the number of data points of the line profile.

The histogram graph for MnO_2 and $ZnMn_2O_4$ thin films was shown in Fig. 6a and b.

Photoluminescence spectroscopy: Photoluminescence is the spontaneous emission of light from a material under optical excitation. Photoluminescence studies provide information of different energy states available between valence and conduction bands responsible for radioactive recombination. Figure 7 shows the PL spectra of undoped MnO_2 and $ZnMn_2O_4$ thin film samples. For both films, a strong and sharp peaks excited at 231 nm was observed. The additional small

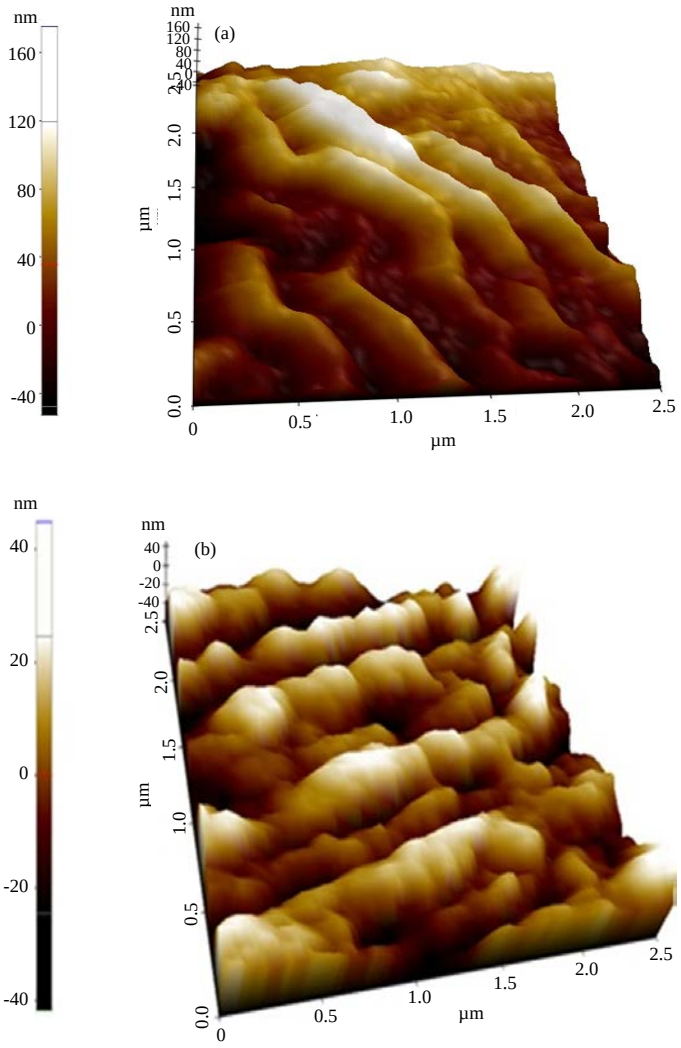

Fig. 5(a-b): AFM image for (a) MnO_2 film and (b) $ZnMn_2O_4$ film

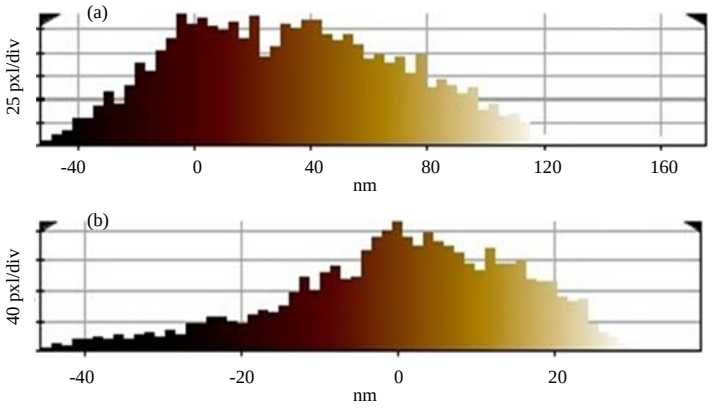

Fig. 6(a-b): Histogram graph for (a) MnO_2 and (b) $ZnMn_2O_4$ thin films

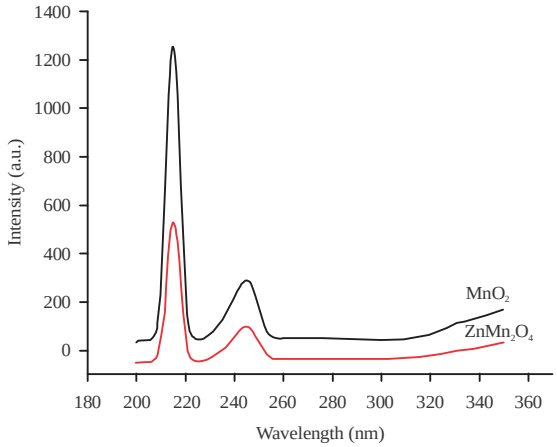

Fig. 7: Photoluminescence spectra of MnO_2 and $ZnMn_2O_4$ thin film

peaks emitted at 245 nm for both MnO_2 and films $ZnMn_2O_4$. However, the intensity of the of the undoped MnO_2 is high compared to $ZnMn_2O_4$ film.

CONCLUSION

From the XRD pattern for the undoped MnO_2 thin films, it was clearly shown that the highly oriented peak is (110) plane due to the annealing process. They belongs to polycrystalline in nature. The grain size was calculated using the scherer formula. For the $ZnMn_2O_4$ thin films were polycrystalline in nature. The crystallinity of the deposited $ZnMn_2O_4$ thin films was improved due to the annealing process. Their grain size was calculated by using the scherer formula and they were found to be decreased. Due to the narrow peak in the undoped MnO_2, the grain size was increased here and their absorbance will be decreased. Finally, there was an increase in their transmittance. The transmittance for the undoped MnO_2 was obtained in the range of 40%. The band gap for the MnO_2 films was found to be 2.4 eV. Due to the broadening of the peaks in the $ZnMn_2O_4$ films, their grain size was decreased here, therefore their absorbance was increased and there was an increase in their transmittance. By the addition of ZnO with MnO_2, the transmittance of $ZnMn_2O_4$ was increased upto 80%. This is due to the addition of ZnO with MnO_2, because ZnO is a window material and they increased the transparency. The band gap for $ZnMn_2O_4$ films was found to be 2.6 eV. Comparing both the MnO_2 and $ZnMn_2O_4$ films, the band gap was increased to the $ZnMn_2O_4$ films. For the undoped MnO_2 thin films, it was clearly observed from the AFM that there is an increase in their grain size. The grain size was increased here and this is due to the annealing effect. In the case of $ZnMn_2O_4$ thin films, from the AFM, we can see that the grain size was decreased. Surface kurtosis value for both the films, which is approximately equal to three. This indicates that for both the deposited films have sharp peak. Surface skewness value for both the films was found to be nearly equal to zero. This shows that both the deposited films were found to be symmetry. The electrical studies were studied using four probe method. It shows that there is an increase in the resistivity, when temperature was increased. This shows the conducting state of the material. After the transition temperature, the resistance of the MnO_2 film starts to decrease along with the increase of their temperature, this is due to the presence of negative temperature coefficient. This shows that the material is a semiconductor. The FESEM for the $ZnMn_2O_4$ thin films, confirms that the decrease in the grain size. It shows that they are well-connected grains.

REFERENCES

Bhide, V.G., R.V. Damle and R.H. Dani, 1959. Dielectric hysteresis in pyrolusite. Physica, 25: 579-580.

Chandru, R.A., S. Patra, C. Oommen, N. Munichandraiah and B.N. Raghunandana, 2012. Exceptional activity of mesoporous β-MnO_2 in the catalytic thermal sensitization of ammonium perchlorate. J. Mater. Chem., 22: 6536-6538.

Cheng, G., L. Yu, T. Lin, R. Yang and M. Sun *et al*., 2014. A facile one-pot hydrothermal synthesis of β-MnO_2 nanopincers and their catalytic degradation of methylene blue. J. Solid State Chem., 217: 57-63.

Duan, Y., H. Ma, X. Li, S. Liu and Z. Ji, 2010. The microwave electromagnetic characteristics of manganese dioxide with different crystallographic structures. Phys. B: Condens. Matter, 405: 1826-1831.

Farid Ul Islam, A.K.M., R. Islam and K.A. Khan, 2005. Effects of deposition variables on spray-deposited MnO_2 thin films prepared from $Mn(C_2H_3O_2)_2.4H_2O$. Renewable Energy, 30: 2289-2302.

Farid Ul Islam, A.K.M., R. Islam, K.A. Khan and Y. Yamamoto, 2007. Temperature effect on the electrical properties of pyrolytic MnO_2 thin films prepared from $Mn(C_2H_3O_2)_2.4H_2O$. Renewable Energy, 32: 235-247.

Fau, P., J.P. Bonino and A. Rousset, 1994. Electrical properties of sputtered MnO_2 thin films. Applied Surface Sci., 78: 203-210.

Ferraris, G., G. Fierro, M.L. Jacono, M. Inversi and R. Dragone, 2002. A study of the catalytic activity of cobalt-zinc manganites for the reduction of NO by hydrocarbons. Applied Catal. B: Environ., 36: 251-260.

Fierro, G., M.L. Jacono, R. Dragone, G. Ferraris, G.B. Andreozzi and G. Graziani, 2005. Fe-Zn manganite spinels and their carbonate precursors: Preparation, characterization and catalytic activity. Applied Catal. B: Environ., 57: 153-165.

Guillemet-Fritsch, S., C. Chanel, J. Sarrias, S. Bayonne, A. Rousset, X. Alcobe and M.L.M. Sarrion, 2000. Structure, thermal stability and electrical properties of zinc manganites. Solid State Ionics, 128: 233-242.

Guo, L.W., D.L. Peng, H. Makino, T. Hanada and S.K. Hong *et al*., 2001. Structural characteristics and magnetic properties of λ-MnO_2 films grown by plasma-assisted molecular beam epitaxy. J. Applied Phys., 90: 351-354.

Hao, Q., L. Xu, G. Li, Z. Ju, C. Sun, H. Ma and Y. Qian, 2011. Synthesis of MnO/C composites through a solid state reaction and their transformation into MnO_2 nanorods. J. Alloys Comp., 509: 6217-6221.

Huang, M.H., S. Mao, H. Feick, H. Yan and Y. Wu *et al*., 2001. Room-temperature ultraviolet nanowire nanolasers. Science, 292: 1897-1899.

Inoue, Y., M. Okamoto and J. Morimoto, 2006. Superimposed emissions on enhanced green emission from zno: Pr powders by evacuated sealed silica tube method. Jpn. J. Applied Phys., 45: 4128-4130.

Jin, Z.W., Y.Z. Yoo, T. Sekiguchi, T. Chikyow and H. Ofuchi *et al*., 2003. Blue and ultraviolet cathodoluminescence from Mn-doped epitaxial ZnO thin films. Applied Phys. Lett., 83: 39-41.

Kind, H., H. Yan, B. Messer, M. Law and P. Yang, 2002. Nanowire ultraviolet photodetectors and optical switches. Adv. Mater., 14: 158-160.

Komaba, S., A. Ogata and T. Tsuchikawa, 2008. Enhanced supercapacitive behaviors of birnessite. Electrochem. Commun., 10: 1435-1437.

Koops, C.G., 1951. On the dispersion of resistivity and dielectric constant of some semiconductors at audiofrequencies. Phys. Rev., 83: 121-124.

Li, Q., Y. Wang and G. Luo, 1999. pH-response of nanosized MnO_2 prepared with solid state reaction route at room temperature. Sensors and Actuators B: Chem., 59: 42-47.

Long, J.W., L.R. Qadir, R.M. Stroud and D.R. Rolison, 2001. Spectroelectrochemical investigations of cation-insertion reactions at sol-gel-derived nanostructured, mesoporous thin films of manganese oxide. J. Phys. Chem. B, 105: 8712-8717.

Look, D.C., 2001. Recent advances in ZnO materials and devices. Mater. Sci. Eng., B80: 383-387.

Ma, S.B., K.W. Nam, W.S. Yoon, X.Q. Yang, K.Y. Ahn, K.H. Oh and K.B. Kim, 2008. Electrochemical properties of manganese oxide coated onto carbon nanotubes for energy-storage applications. J. Power Sources, 178: 483-489.

Minami, T., T. Shirai, T. Nakatani and T. Miyata, 2000. Electroluminescent devices with Ga_2O_3: Mn thin-film emitting layer prepared by sol-gel process. Jpn. J. Applied Phys., 39: L524-L526.

Rizzi, G.A., R. Zanoni, S. Di Siro, L. Perriello and G. Granozzi, 2000. Epitaxial growth of MnO nanoparticles on Pt(111) by reactive deposition of Mn_2 $(CO)_{10}$. Surface Sci., 462: 187-194.

Sakohara, S., L.D. Tickanen and M.A. Anderson, 1992. Luminescence properties of thin zinc oxide membranes prepared by the sol-gel technique: Change in visible luminescence during firing. J. Phys. Chem., 96: 11086-11091.

Xiao, L., Y. Yang, J. Yin, Q. Li and L. Zhang, 2009. Low temperature synthesis of flower-like $ZnMn_2O_4$ superstructures with enhanced electrochemical lithium storage. J. Power Sour., 194: 1089-1093.

Yang, Y.Y., Y.Q. Zhao, L.F. Xiao and L.Z. Zhang, 2008. Nanocrystalline $ZnMn_2O_4$ as a novel lithium-storage material. Electrochem. Commun., 10: 1117-1120.

Zhai, D., B. Li, C. Xu, H. Du, Y. He, C. Wei and F. Kang, 2011. A study on charge storage mechanism of α-MnO_2 by occupying tunnels with metal cations (Ba^{2+}, K^+). J. Power Sources, 196: 7860-7867.

Zheng, D., S. Sun, W. Fan, H. Yu and C. Fan *et al*., 2005. One-step preparation of single-crystalline β-MnO_2 nanotubes. J. Phys. Chem. B, 109: 16439-16443.

Zhou, J., N. Xu and Z.L. Wang, 2006. Dissolving behavior and stability of ZnO wires in biofluids: A study on biodegradability and biocompatibility of ZnO nanostructures. Adv. Mater., 18: 2432-2435.

Zu, P., Z.K. Tang, G.K.L. Wong, M. Kawasaki, A. Ohtomo, H. Koinuma and Y. Segawa, 1997. Ultraviolet spontaneous and stimulated emissions from ZnO microcrystallite thin films at room temperature. Solid State Commun., 103: 459-463.